JOURNAL OF GEOPHYSICAL RESEARCH, VOL. 112, A05104, doi:10.1029/2006JA011904, 2007

Prediction of the 1-AU arrival times of CME-associated interplanetary shocks: Evaluation of an empirical interplanetary shock propagation model

K.-H. Kim,[1] Y.-J. Moon,[1] and K.-S. Cho[1]

Received 8 June 2006; revised 10 November 2006; accepted 17 January 2007; published 17 May 2007.

[1] The traveltimes of interplanetary (IP) shocks at 1 AU associated with coronal mass ejections (CMEs) can be predicted by the empirical shock arrival (ESA) model of Gopalswamy et al. [2004] based on a constant IP acceleration. We evaluate the ESA model using 91 IP shocks identified from sudden commencement (SC)/sudden impulse (SI) on the Earth and by examining the solar wind data from the ACE and WIND satellites during the period of 1997 to 2002. Out of 91 CME-IP shock pairs, 55 events (~60%) were predicted within ±12 hours from the ESA model. The ESA model predicted ~59% (43 out of 73) of the events during solar maximum (1999–2002) and ~67% (12 out of 18) of the events during solar minimum (1997–1998) within ±12 hours from the predicted curve. Comparing the predicted (T_{mod}) and observed (T_{obs}) shock arrival times during solar maximum, we find that the deviations ($\Delta T = T_{obs} - T_{mod}$) of shock arrival times from the ESA model strongly correlate with the CME initial speeds (V_{CME}) (linear correlation, $r = 0.77$). Such a strong correlation indicates that the constant IP acceleration in the ESA model is not reasonably well applied for all V_{CME}. From the linear regression analysis, we obtain a linear fit to the relationship ($r = -0.62$) between IP shock traveltime T (in hours) and V_{CME} (in kilometer per second) during the solar maximum, which can be expressed as $T = 76.86 - 0.02V_{CME}$. In addition, we find that the IP shocks associated with the fast CMEs corresponding to strong SC/SI events have short traveltimes compared with other fast CMEs and that there is a negative correlation between the SC/SI strength and the IP shock traveltime. We suggest that this negative correlation is due to not only the V_{CME} but also the CME mass/density and discuss the influence of the mass/density of CME on the arrival time of IP shock at 1 AU.

Citation: Kim, K.-H., Y.-J. Moon, and K.-S. Cho (2007), Prediction of the 1-AU arrival times of CME-associated interplanetary shocks: Evaluation of an empirical interplanetary shock propagation model, *J. Geophys. Res.*, *112*, A05104, doi:10.1029/2006JA011904.

1. Introduction

[2] Coronal mass ejections (CMEs) are the largest and most energetic solar eruption phenomena arising from a destabilization of the coronal magnetic configurations. When CMEs are launched from the Sun, they travel through interplanetary space and, if directed toward the Earth, impinge on the Earth's magnetosphere. Such interplanetary CMEs (ICMEs) can trigger severe geomagnetic disturbances 1 to 5 days after CMEs originate from the Sun. Therefore it is important to make a prediction of the arrival time of geo-effective CMEs at 1 AU for space weather forecasting.

[3] The CME speeds near the Sun are in the range of ~100–2000 km/s [*Yashiro et al.*, 2004], while near the Earth, they lie in a narrower range comparable to the solar wind speed [e.g., *Gopalswamy et al.*, 2000; *Cane and Richardson*, 2003]. This indicates that CMEs interact with the ambient solar wind and experience a prolonged acceleration or deceleration toward the solar wind speed as they propagate to the Earth. If we know the relationship between the CME initial speed at the Sun and the corresponding ICME speed at 1 AU, we can make a prediction of CME transit times from the Sun to 1 AU. This has been done by *Gopalswamy et al.* [2000, 2001a]. The authors found that CMEs are subject to a constant interplanetary (IP) acceleration that depends linearly on the CME initial speed. In the empirical CME arrival model by Gopalswamy et al., the constant IP acceleration was obtained from the CME initial speed, the ICME speed, and the transit time of the CME to 1 AU. However, there were few fast CME events in their studies; that is, most of the CME initial speeds were below 1200 km/s. Therefore it is questionable whether the constant IP acceleration can be applied to fast CMEs.

[4] IP forward shocks (hereinafter referred to as IP shocks) are often driven by CMEs. They are clearly identified by in situ solar wind observations having a sharp increase in the interplanetary magnetic field and solar wind

[1]Korea Astronomy and Space Science Institute, Daejeon, South Korea.

0148-0227/07/2006JA011904$09.00

speed and density. When CME-associated IP shocks impact the magnetopause, the magnetosphere is compressed. At the same time, fast-mode magnetohydrodynamic waves are generated at the magnetopause and then propagate toward the Earth. When they arrive on the ground, a step-like increase in the horizontal *H* component (magnetically northward) at low latitude is observed. These signatures are called sudden commencements (SC) if a geomagnetic storm follows and sudden impulse (SI) events otherwise [*Araki*, 1994]. Since an IP shock front is ahead of the main part of the ICME, the shock arrival time implies the earliest geomagnetic disturbance.

[5] Recently, *Gopalswamy et al.* [2004] provided an empirical model to predict the 1-AU arrival of IP shocks. The IP shock model is extended from the empirical CME arrival model of *Gopalswamy et al.* [2001a] based on a constant IP acceleration. A comparison of CME and/or IP shock propagation models has been summarized well in recent studies [e.g., *McKenna-Lawlor et al.*, 2002; *Cho et al.*, 2003; *Owens and Cargill*, 2004]. In this study, we examine the traveltimes of CME-associated IP shocks and evaluate the empirical shock arrival model of *Gopalswamy et al.* [2004]. We will show that there is a systematic dependence of the IP shock traveltime deviations from the empirical shock arrival model with respect to the CME initial speeds. This indicates that the constant IP acceleration in the empirical model is not well applied for all CMEs. The propagation properties of IP shocks with respect to the CME initial speed and CME mass will be discussed below.

2. Data and Event Selection

[6] In this paper, we examine the propagation of IP shocks observed during the period of 1997 to 2002 and evaluate the empirical shock arrival model [*Gopalswamy et al.*, 2004] to predict the arrival of IP shocks at 1 AU. The IP shocks are associated with white light CMEs observed by the SOHO/LASCO coronagraphs. The CME initial speed has been measured by tracking the same CME feature (leading edge) in each frame, which is a critical input parameter to the empirical shock arrival model, and CME onset times are obtained from the CME catalog [*Yashiro et al.*, 2004]. To determine if CME-associated IP shocks arrive at the Earth, we use the occurrence of SC/SI events identified in the 1-min resolution SYM-H index data [*Iyemori and Rao*, 1996]. The SC/SI events are defined as a rapid increase in SYM-H values with more than 5 nT within 10 min. We also use the solar wind data from the Wind spacecraft for the events during the period of January 1997 to February 1998 and from the ACE spacecraft during the period of March 1998 to December 2002 to confirm the 1-AU arrival of the IP shocks. We note that the solar wind data for the IP shock event on 24 November 2001 are not available from ACE. However, the wind data have provided the solar wind speed and density for the event.

[7] We analyze 91 CME-IP shock pairs in the time period from 1997 to 2002. The events are mostly selected from the published archival data in the studies of the interplanetary CME (ICME) and IP shock propagations by *Cane and Richardson* [2003] and *Manoharan et al.* [2004]. Table 1 presents the list of the CME-associated SC/SI events used in both studies and the 11 events that were not listed in both studies. We note that the SC/SI events are associated with halo or partial halo CMEs, which have the azimuthal extent of 360° or >120° in the LASCO field of view [*Yashiro et al.*, 2004].

[8] In order to avoid any ambiguity in the identification of CME-IP shock (SC/SI) pair, we have applied specific criteria. If the ICMEs in the studies of *Cane and Richardson* [2003] and *Manoharan et al.* [2004] have no clear SC/SI signatures, we do not include the ICME events in this study. In some cases, both studies disagree on the correspondence of 1-AU signatures and solar sources of CMEs. Some SC/SI events are identified to be associated with halo or partial halo CMEs. However, the CME events are not classified as halo or partial halo CME in the paper of *Yashiro et al.* [2004]. Those events are marked by "?" in columns 2 and 4 for CME ambiguity and in columns 5, 9 and 10 for SC/SI ambiguity. They are not included in this study. Multiple SC/SI events occurred on 26 November 2000, and they are probably the result of multiple CMEs on 24–25 November 2000. These multiple SC/SI events are difficult to identify in one-to-one correspondences between the CMEs on the Sun and the SC/SI events on the Earth. Both previous studies included such events. In this study, however, we exclude the SC/SI events when their source identification is ambiguous. Such multiple SC/SI events are marked by "M" in column 9.

3. Observations

[9] The CME-associated IP shock traveltimes at 1 AU are plotted in Figure 1 as a function of the initial speed of the corresponding CME. The solid curve and two dashed curves indicate the IP shock traveltimes predicted by the empirical shock arrival (ESA) model [*Gopalswamy et al.*, 2004] and a deviation of 12 hours from the prediction curve, respectively. The ESA model is extended from the empirical CME arrival (ECA) model of *Gopalswamy et al.* [2001a], assuming that a constant acceleration ceases over a certain distance. In this study, the acceleration cessation distance of 0.76 AU is assumed to predict the IP shock arrivals because it makes a best prediction curve for the measured CME traveltimes [*Gopalswamy et al.*, 2001a]. The IP shock arrival time in the ESA model is obtained by simply shifting the CME arrival time in the ECA model in accordance with the standoff distance, which is given by the difference between the positions of a shock driven by CME and the leading edge of the CME [*Gopalswamy et al.*, 2004].

[10] Figure 1a shows the 91 events observed during the period of 1997 to 2002. The solid circles indicate the events within ±12 hours from the ESA model curve. The ESA model predicts 55 (∼60%) of the 91 events within ±12 hours. Since the 12-hour deviation from the ESA model is comparable to the mean error of 10.7 hours for the ECA model, we consider the events within ±12 hours as well-predicted events. This percentage rate is higher than the prediction percentage rate (∼52%) by using the ESA model in the work of *Manoharan et al.* [2004]. We note that the data used in this study and those in the paper of Manoharan et al. come from the same time period (1997–2002). However, the selected events in this study are not the same as those in the report of Manoharan et al. because of slightly different identification of the CME-IP shock pairs as mentioned in section 2.

Table 1. List of IP Shocks, SC/SI Events, and Associated CMEs[a]

LASCO CME				IP Shock				SC/SI		
Date	Time, hhmm	V_{CME}, km/s	H/P	Date	Time, hhmm	V_{SW2}, km/s	V_{SW1}, km/s	Time, hhmm	ΔH, nT	Ref.
6 January 1997	1510	136	H	10 January 1997	0052	403	384	0104	12	1, 2
7 February 1997	0030	490	H	9 February 1997	1250	593	514	1321	15	1, 2
12 May 1997	0530	464	H	15 May 1997	0115	386	318	0159	31	1, 2
21 May 1997	2100	296	P	25 May 1997	1351	320	296	1434	15	1
30 July 1997	0445	104	H	3 August 1997					?	1
30 August 1997	0130	371	H	2 September 1997	2237	352	324	2259	13	1, 2
17 September 1997	2028	377	H	21 September 1997				?		1, 2
28 September 1997	0108	359	H	1 October 1997	–	–	–	0059	28	1
6 October 1997	1528	293	P	10 October 1997	1557	433	406	1612	11	1
23 October 1997	1126	503	H	26 October 1997					?	1
4 November 1997	0610	785	H	6 November 1997	–	–	–	2248	47	1
19 November 1997	1227	150	H	22 November 1997	0913	439	347	0949	40	1, 2
6 December 1997	1027	397	P	10 December 1997	0433	362	290	0526	28	1
26 December 1997	0232	197	P	30 December 1997	0113	369	322	0209	15	1, 2
2 January 1998	2328	438	H	6 January 1998	1327	371	307	1416	22	1
17 January 1998	0409	350	H	21 January 1998					?	1
25 January 1998	1526	693	H	28 January 1998	1557	395	370	1640	14	1, 2
14 February 1998	0655	123	P	?						1, 2
28 February 1998	1248	176	P	4 March 1998	1058	379	353	1156	7	1, 2
2 April 1998	1830	155	?	7 April 1998	1650	337	286	1749	17	2
29 April 1998	1659	1374	H	1 May 1998	2123	575	487	2156	40	1, 2
2 May 1998		938	H	4 May 1998				M		1, 2
21 June 1998	0535	192	P	?						1, 2
15 October 1998	1004	262	H	18 October 1998	1901	357	321	1952	19	1, 2
4 November 1998	0754	523	H	7 November 1998	0737	445	411	0815	18	2
5 November 1998	2044	1118	H	8 November 1998	0421	587	491	0451	7	1, 2
9 November 1998	1818	325	P	?						1, 2
7 March 1999	0554	835	?	10 March 1999	0038	442	407	0130	12	2
13 April 1999	0330	291	H	16 April 1999	1035	458	376	1125	15	1, 2
24 June 1999	1331	975	H	26 June 1999	1925	394	336	2016	33	1
29 June 1999	0731	634	H	2 July 1999	0023	561	486	0059	21	2
3 July 1999	1954	536	P	6 July 1999	1416	390	340	1509	16	1
28 July 1999	0906	462	H	31 July 1999	1740	599	590	1827	19	1
1 August 1999	1927	1159	P	4 August 1999	0115	370	328	0219	20	2
12 September 1999	0054	732	P	15 September 1999	0719	600	544	0753	14	–
13 September 1999	1731	444	P	15 September 1999	1941	595	560	2019	15	2
20 September 1999	0606	604	H	22 September 1999	1146	426	382	1222	23	1, 2
18 October 1999	?		?	?						1, 2
25 October 1999	1426	511	P	28 October 1999	1127	416	380	1216	12	2
18 January 2000	1754	739	H	22 January 2000	0023	354	328	0109	9	1, 2
8 February 2000	0930	1079	H	11 February 2000	0209	531	417	0258	18	1, 2
10 February 2000	0230	944	H	11 February 2000	2319	595	460	2352	36	1, 2
12 February 2000	0431	1107	H	14 February 2000	0656	643	569	0731	14	1, 2
17 February 2000	2006	728	H	20 February 2000	2045	385	343	2139	29	1, 2
4 April 2000	1632	1188	H	6 April 2000	1603	536	388	1639	46	1
2 June 2000	1030	442	?							2
6 June 2000	1554	1119	H	8 June 2000	0841	759	523	0910	59	1, 2
10 June 2000	1708	1108	H	12 June 2000	2140	538	455	2208	17	–
20 June 2000	0910	464	P	23 June 2000	1227	505	390	1303	36	2
7 July 2000	1026	453	H	10 July 2000	0557	489	404	0638	27	1, 2
8 July 2000	2350	483	?							2
11 July 2000	1327	1078	H	13 July 2000	0904	610	508	0942	26	1
14 July 2000	1054	1674	H	15 July 2000	1438	–	–	1438	69	1, 2
24 July 2000	2354	320	?							2
25 July 2000	0330	528	H	28 July 2000	0542	450	346	0634	29	1
6 August 2000	?							?		1, 2
9 August 2000	1630	702	H	11 August 2000	1811	538	431	1845	17	1,2
4 September 2000	0606	849	P	6 September 2000	1614	482	397	1700	32	–
12 September 2000	1154	1550	H	15 September 2000	0400	–	316	0449	22	2
16 September 2000	0518	1215	H	17 September 2000				?		2
2 October 2000	0350	525	H	5 October 2000	0240	456	363	0326	27	–
2 October 2000	2026	569	H	5 October 2000				?		1, 2
9 October 2000	2350	798	H	12 October 2000	2145	439	324	2228	25	1, 2
25 October 2000	0826	770	H	28 October 2000	0908	430	371	0954	25	1
1 November 2000	1626	801	H	4 November 2000	0134	411	362	0221	20	–
3 November 2000	1826	291	H	6 November 2000	0915	611	483	0948	15	2
8 November 2000	2306	1738	P	10 November 2000	–	–	–	0624	60	1
1 November 2000				26 November 2000				M		1
20 January 2001	2130	1507	H	23 January 2001	1005	533	418	1048	32	1
15 February 2001	1354	625	H	20 February 2001				?		2
28 February 2001	1450	313	P	3 March 2001	1039	510	443	1121	13	1, 2
16 March 2001	0350	271	P	19 March 2001	1022	372	330	1114	17	1, 2

Table 1. (continued)

LASCO CME				IP Shock				SC/SI		
Date	Time, hhmm	V_{CME}, km/s	H/P	Date	Time, hhmm	V_{SW2}, km/s	V_{SW1}, km/s	Time, hhmm	ΔH, nT	Ref.
19 March 2001	0526	360	H	22 March 2001	1241	351	300	1340	22	2
24 March 2001	2050	906	H	27 March 2001	0109	428	346	0143	28	–
25 March 2001	1706	677	H	27 March 2001	1715	506	422	1747	23	1, 2
29 March 2001	1026	942	H	31 March 2001				?		1, 2
5 April 2001	1706	1390	H	7 April 2001	1700	540	444	1732	21	–
6 April 2001	1930	1270	H	8 April 2001	1031	636	500	1101	50	1
9 April 2001	1554	1192	H	11 April 2001	1313	602	512	1343	15	–
11 April 2001	1331	1103	H	13 April 2001	0707	646	522	0734	18	1, 2
15 April 2001	1406	1199	P	18 April 2001	0005	485	377	0046	40	–
19 April 2001	1230	392	P	21 April 2001	1505	400	354	1600	16	2
26 April 2001	1230	1006	H	28 April 2001	0430	776	468	0500	57	1, 2
15 June 2001	1556	1701	H	18 June 2001	0155	344	323	0259	32	–
9 August 2001	1030	479	P	12 August 2001	1047	340	400	1131	35	2
14 August 2001	1601	618	H	17 August 2001	1016	481	346	1103	33	1
25 August 2001	1650	1433	H	27 August 2001	1919	545	449	1952	42	1
27 August 2001	1726	408	?	30 August 2001					?	2
11 September 2001	2130	646	P	14 September 2001	0117	433	372	0204	27	2
27 September 2001	0454	509	P	29 September 2001	0906	613	563	0940	22	1, 2
28 September 2001	0854	846	H	30 September 2001	1846	548	469	1924	23	1, 2
9 October 2001	1130	973	H	11 October 2001	1620	476	383	1701	36	1, 2
19 October 2001	1650	901	H	21 October 2001	1612	570	404	1648	35	1, 2
22 October 2001	1506	1336	H	25 October 2001	0802	454	367	0848	33	2
25 October 2001	1526	1092	H	28 October 2001	0243	513	352	0319	35	2
29 October 2001	1150	598	?							2
4 November 2001	1635	1810	H	6 November 2001	–	–	–	0152	87	1, 2
17 November 2001	0530	1379	H	19 November 2001	1735	545	454	1815	24	1
22 November 2001	2330	1437	H	24 November 2001	0550	960	713	0555	83	1
26 November 2001	0530	1446	P	29 December 2001	0446	429	367	0538	50	1
12 February 2002	?		?							1
14 February 2002	0230	473	P	17 February 2001	0209	391	367	0255	27	2
15 March 2002	2306	957	H	18 March 2002	1236	438	350	1322	62	1, 2
20 March 2002	1754	603	P	23 March 2002	1053	460	399	1137	25	1, 2
15 April 2002	0350	720	H	17 April 2002	1021	456	347	1107	64	2
17 April 2002	0826	1240	H	19 April 2002	0835	571	447	0835	38	1
7 May 2002	0406	720	H	10 May 2002	1030	412	364	1030	32	2
8 May 2002	1350	614	H	11 May 2002	0925	424	358	1014	32	2
17 May 2002	0127	461	?							2
22 May 2002	M			23 May 2002				M		1
15 July 2002	2130	1300	H	17 July 2002	1525	476	409	1604	44	1, 2
18 July 2002	M									2
29 July 2002	1207	562	P	1 August 2002	0422	500	392	0509	24	2
29 July 2002	2330	360	P	1 August 2002	2218	462	430	2309	37	2
16 August 2002	1230	1459	H	18 August 2002	1810	515	421	1846	47	1, 2
17 August 2002	2230	254	?							2
5 September 2002	1654	1657	H	7 September 2002	1609	546	391	1636	15	1, 2
17 September 2002	?									1
6 November 2002	0606	485	?							2
24 November 2002	2030	1077	H	26 November 2002	2110	505	405	2150	34	–

[a]Column 3: CME initial speed (V_{CME}). Column 7: Postshock solar wind speed (V_{SW2}). Column 8: Preshock solar wind speed (V_{SW1}). Column 10: SC/SI amplitude (ΔH). Column 11: "1" indicates the CME events in the study of *Cane and Richardson* [2003] and "2" indicates the CME events in the work of *Manoharan et al.* [2004].

[11] We have compared the CME events observed under different solar activity levels. Figure 1b shows the events during solar minimum (1997–1998), and the events during solar maximum from early phase of solar maximum (1999) to late phase of solar maximum (2002) are plotted in Figure 1c. The ESA model predicts ~67% (12 out of 18 events) and ~59% (43 out of 73 events) within ±12 hours for solar minimum and solar maximum, respectively. Although the total number (18) of events during solar minimum is not so large, we find that there is a tendency for the CME initial speed (V_{CME}) to increase toward solar maximum. Such a V_{CME} dependence on the solar cycle is consistent with the result of a statistical study reported by *Yashiro et al.* [2004]. More detailed annual variations of CME properties can be found in their study.

[12] The data points in Figure 1 provide an insight into the propagation properties of IP shocks with respect to V_{CME}. First, the slow CMEs (V_{CME} < 500) during solar minimum are scattered around the ESA model curve. Second, there is a tendency for the ESA model to overestimate (underestimate) traveltimes of the events with V_{CME} < 700 (>1000) km/s during solar maximum. Third, the IP shock events associated with V_{CME} >1300 km/s during solar maximum have a large deviation (~17–42 hours) from the ESA model except for four data points at V_{CME} = 1437, 1674, 1738, and 1810 km/s. These four data points reside close to the ESA model curve. If the constant IP acceleration in the

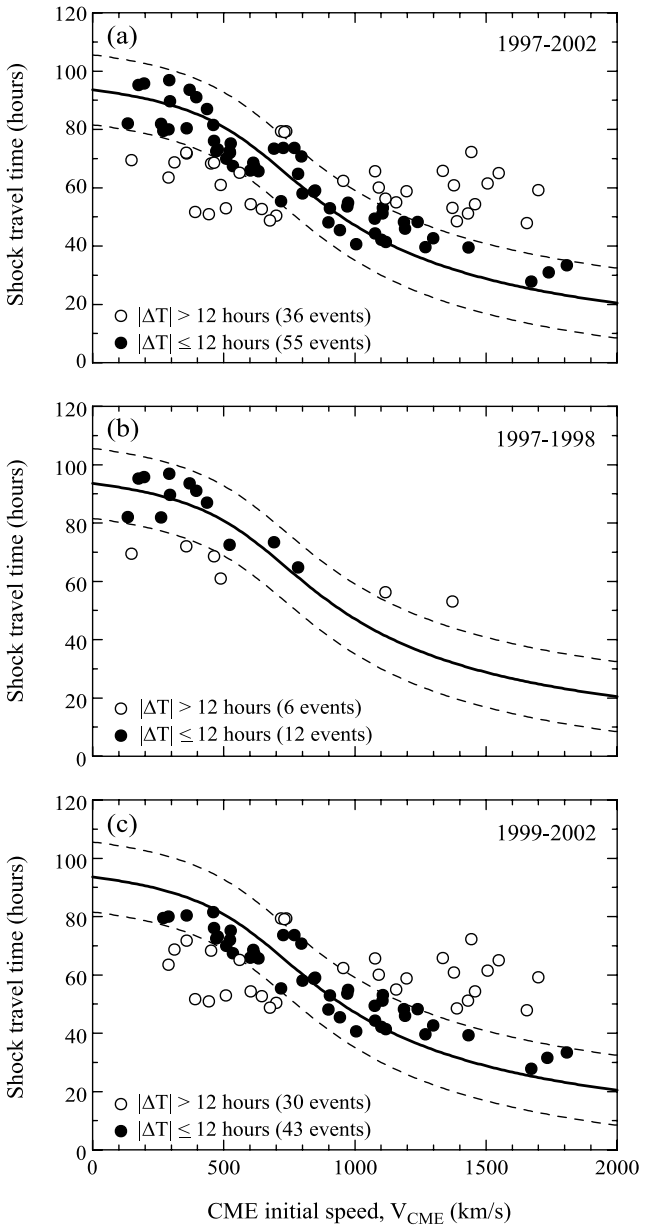

Figure 1. IP shock traveltimes to 1 AU as a function of the CME initial speed during (a) 1997–2002, (b) solar minimum (1997–1998), and (c) solar maximum (1999–2002). In each panel, the solid curve is the empirical shock arrival (ESA) model prediction from the study of *Gopalswamy et al.* [2004]. ΔT is a deviation from the ESA model. The ±12-hour deviations from the ESA model curve are given by the dashed lines.

ECA model is reasonably well applied for all V_{CME}, we would expect that all of the data points should be around the predicted curve of the ESA model. However, there are large positive (negative) deviations for most of (some of) the events with V_{CME} >1300 km/s (<700 km/s) in Figure 1c, indicating that we need to be careful to apply the constant IP acceleration for V_{CME} < 700 km/s and V_{CME} >1300 km/s during solar maximum. Such positive and negative deviations with respect to V_{CME} could be explained with a systematic V_{CME} dependence of the deviations.

[13] In order to examine whether there is a systematic dependence of IP shock traveltime deviations from the ESA model, we compare the predicted (T_{mod}) and observed (T_{obs}) shock arrival times. Since the number of the events during solar minimum is not so large and the CME initial speeds corresponding to the events do not cover a wide range, we focus on the events during solar maximum to examine the relationship between V_{CME} and IP shock arrival times. Figure 2 shows the scatterplot of the deviations ($\Delta T = T_{obs} - T_{mod}$) of shock arrival times from the ESA model for V_{CME} during solar maximum. In this plot, we include a straight line $y = a + bx$ determined by the least squares fitting, the linear correlation coefficient (r), the standard deviation (δ), and the number of samples (n). The open circles in Figure 2 indicate the events associated with the CMEs interacting with the preceding CME(s) identified by *Manoharan et al.* [2004].

[14] There is a clear linear relationship between ΔT and V_{CME} with a correlation coefficient of 0.77. This good positive correlation between the two parameters implies that the constant IP acceleration in the ECA model cannot be applied for the whole V_{CME} range as mentioned above. That is, the fast CMEs (V_{CME} >1300 km/s) decelerate more, and the slow CMEs (V_{CME} < 500 km/s) accelerate more than the constant IP acceleration in the ECA model. We suggest that the constant IP acceleration can be applied for V_{CME} in the range of ~500–1300 km/s during the solar maximum.

[15] Although we find a good correlation between ΔT and V_{CME}, there is a large scatter for a given V_{CME} in a wide range of V_{CME}. One might expect that the large scatter is due to different background solar wind conditions between individual CMEs during their passage from the Sun to the near-Earth space. The simplest approach to confirm the above argument is to examine the relationship between ΔT and $\Delta V1$, which is the difference in V_{CME} and the solar wind speed (V_{SW1}) just before the IP shock, and between ΔT and $\Delta V2$, which is the difference in V_{CME} and the postshock solar wind speed (V_{SW2}). Figures 3a and 3b show

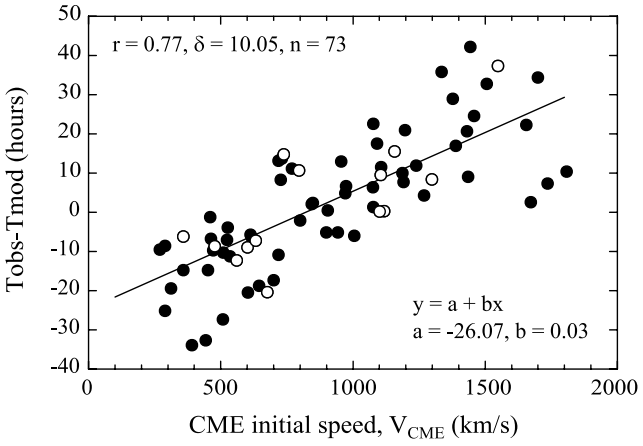

Figure 2. Scatter diagram of deviation ($\Delta T = T_{obs} - T_{mod}$) of shock arrival times from the ESA model versus the CME initial speed during solar maximum (1999–2002). The straight line is determined by the least squares fitting. The linear correlation coefficient r, standard deviation δ, and number of data points n are indicated in the panel. The CME-CME interacting events are plotted with the open circles.

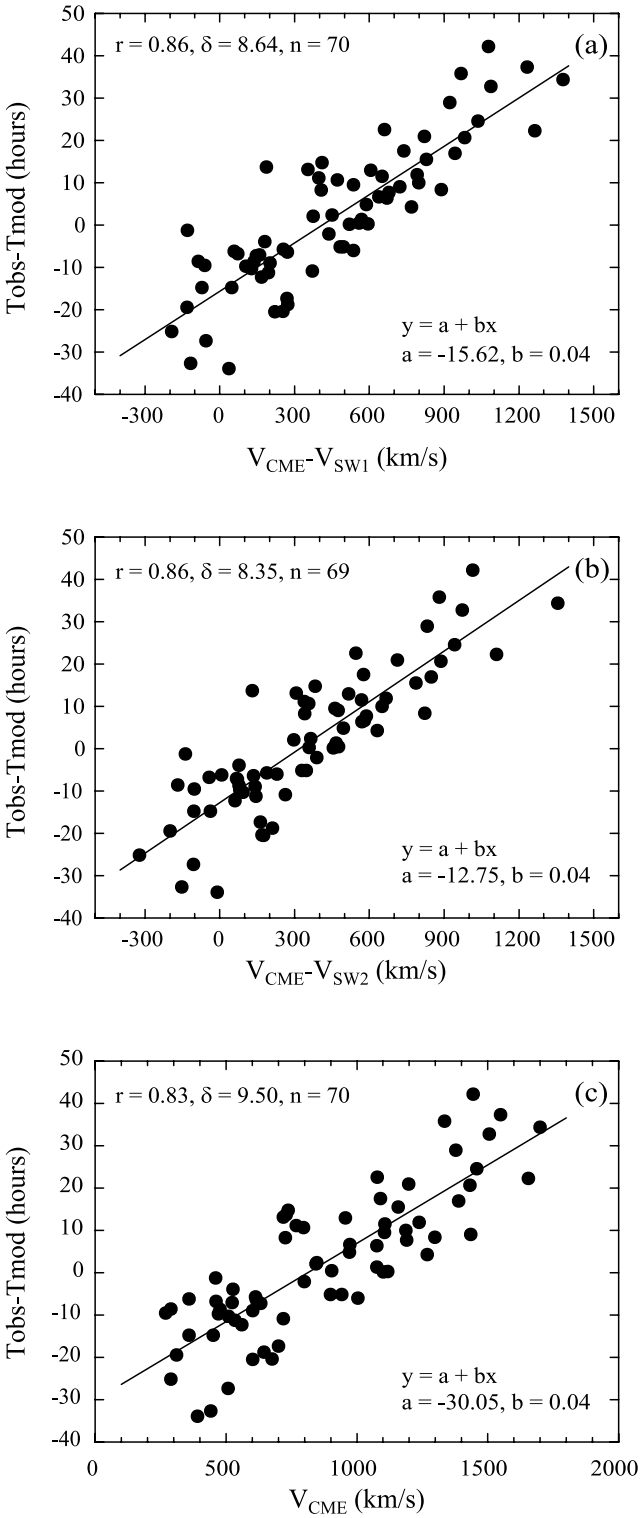

Figure 3. The format is the same as that in Figure 2 except for the horizontal axis parameter, (a) the difference in V_{CME} and the solar wind speed (V_{SW1}) just before the IP shock, and (b) the difference in V_{CME} and the postshock solar wind speed (V_{SW2}). (c) Same as Figure 2 but excluding the three events lying close to the ESA model prediction curve.

the scatterplots of ΔT versus $\Delta V1$ and ΔT versus $\Delta V2$ with the best fit straight lines, respectively. We note that the solar wind data of the exceptional three events with fast CME speed (V_{CME} = 1674, 1738, and 1810 km/s) shown in Figure 1c are not available. In order to make the comparison meaningful, we exclude the three events in the scatter diagram of ΔT versus V_{CME} in Figure 3c. Although the scatter diagrams of Figures 3a and 3b are quite similar to Figure 3c, the correlation coefficient of ΔT-$\Delta V1$ and ΔT-$\Delta V2$ is larger than that of ΔT-V_{CME}, and the standard deviation in Figures 3a and 3b is reduced about the best fit straight line. This indicates that the scatter in ΔT-V_{CME} plot must be partially due to the solar wind interaction with CMEs.

[16] Figure 4 shows the scatterplot of the shock traveltime and V_{CME} during the solar maximum. Least squares fitting of a straight line to the two quantities yields a relationship, $T = 76.86 - 0.02V_{CME}$, where T is the arrival time in hours and V_{CME} is the CME initial speed in kilometer per second. The linear correlation coefficient and the standard deviation are -0.62 and ± 10.23 hours, respectively. Most of the events corresponding to slow and fast CMEs are scattered around the linear fit. The linear fit predicts $\sim$74% within $\pm$12 hours from the straight line. This prediction is about 15% higher than that from the ESA model.

4. Discussion and Summary

[17] In this study, we have examined the ESA model for the prediction of the arrival time of IP shocks associated with halo/partial halo CMEs. The IP shocks passing over the Earth were identified by the SC/SI events measured on ground stations. We compared the onset times of the SC/SI events and their corresponding CMEs. Since the ESA model is extended from the CME arrival model of *Gopalswamy et al.* [2001a] based on a constant IP acceleration, the constant IP acceleration is an important parameter in the ESA model. The authors found that the constant IP acceleration is linearly dependent on the CME initial speed. However, it

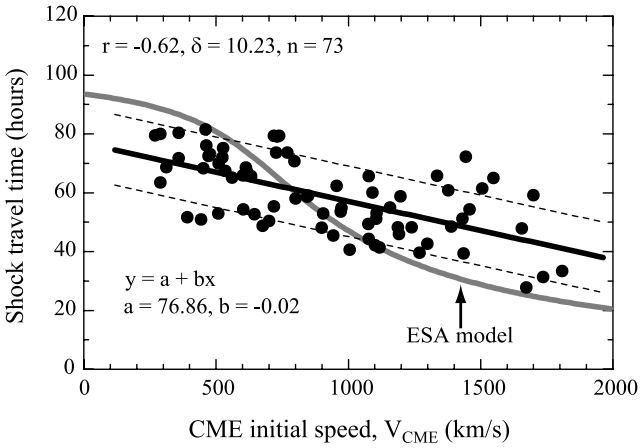

Figure 4. IP shock traveltimes to 1 AU as a function of the CME initial speed during solar maximum. The linear fit to the relationship between shock traveltime and V_{CME}. The gray solid curve is the IP shock arrival time prediction from the ESA model in each panel. The $\pm$12-hour deviations from the linear fit are plotted with the dashed lines.

Table 2. List of CME Sky-Plane Speeds and CME True Speeds

Date	Time, hhmm	V_{CME}, km/s	V_{True}, km/s
29 June 1999	0731	634	698
8 February 2000	0930	1079	1091
17 February 2000	2006	728	668
4 April 2000	1632	1188	1645
6 June 2000	1554	1119	1028
10 June 2000	1708	1108	1460
7 July 2000	1026	453	315
11 July 2000	1327	1078	1753
12 September 2000	1154	1550	1358
2 October 2000	0350	525	578

is questionable whether the constant acceleration can be applied for all initial CME speeds, especially fast CMEs (V_{CME} >1300 km/s), because the number of data points in the work of Gopalswamy et al. is small in the high-speed range. It has been reported that such fast CMEs can give rise to major geomagnetic storms [e.g., *Moon et al.*, 2005; *Srivastava and Venkatakrishnan*, 2004]. Thus it is important to predict the 1-AU arrival of fast CMEs and their associated IP shocks for space weather forecasting.

[18] We have found a systematic dependence of the IP shock traveltime deviations from the ESA model for V_{CME} during solar maximum (1999–2002). This result indicates that the assumption that all the CMEs experience the same IP acceleration given in the ECA model is not valid for slow and fast CMEs. In particular, most of the IP shocks associated with V_{CME} >1300 km/s have a large positive deviation (~17–42 hours) from the ESA model, implying that the fast CMEs experience more deceleration during their propagation from the Sun to the Earth than the constant IP acceleration in the ECA model.

[19] Recently, *Manoharan et al.* [2004] showed large deviations of shock arrival times from the empirical model for slow (V_{CME} <300 km/s) and fast (V_{CME} >800 km/s) CMEs. The authors interpreted the observations with the CME-CME interactions. That is, the slow and fast CMEs go through strong effective acceleration, which is determined by the interaction of CMEs with preceding CME(s). As shown in Figure 2, however, the CME interactions do not play a significant role in determining the systematic dependence of the IP shock traveltime deviations from the ESA model for V_{CME}.

[20] For an improved prediction of the IP shocks associated with slow and fast CMEs, we obtain a linear fit to the relationship between shock traveltime and V_{CME}, $T = 76.86 - 0.02V_{CME}$. Unlike the ESA model for underestimating (overestimating) IP shock transit times of the fast (slow) CMEs, the events are scattered around the linear fit. Approximately 74% of the events are predicted within ±12 hours from the linear fit, which is about 15% higher than the prediction from the ESA model.

[21] As mentioned above, the ESA model is extended from the ECA model of *Gopalswamy et al.* [2001a]. In the ECA model, limb CMEs and data from spacecraft in quadrature were used to minimize projection effects in determining the initial speed of CMEs. In our study, however, we have used the projected speed in the plane of the sky. Therefore one might argue that the main cause for the deviations from the ESA model is due to the projection effects. It is not easy to correct the projection effect of halo CMEs because there is no simple way to obtain the width of halo CME. Recently, *Michalek et al.* [2003] proposed a new method to obtain "true speed(s)" of halo CMEs with sky-plane speeds. From the list of halo CMEs in the paper of *Michalek et al.* [2003], we obtained the true speeds for 10 CMEs causing SC/SI events during the interval from 1999 to 2000. Table 2 presents the list of 10 events.

[22] Figure 5 shows the events associated with the sky-plane speed, which is used as the CME initial speed (V_{CME}) in our study, and the true speed (V_{True}), which is corrected for the projection effect, with the ESA model curve. Although we have small data points, V_{CME} gives better prediction than V_{True}. This result is similar to that in the work of *Gopalswamy et al.* [2001a] (see Figure 6 in their study). This unexpected result may be due to the assumptions: constant CME velocity, symmetric CME, and propagation with constant angular width. *Michalek et al.* [2003] noted that the average corrected speeds are only 20% greater than the sky-plane speeds. *Owens and Cargill* [2004] reported that the removal of the projection effect yields only a minor improvement in the prediction accuracy of the CME transit time. *Gopalswamy et al.* [2001a] suggest that the radial speed is comparable to the sky-plane speed if the CME is expanding rapidly in the beginning and that the sky-plane speed seems to be a reasonable representation of

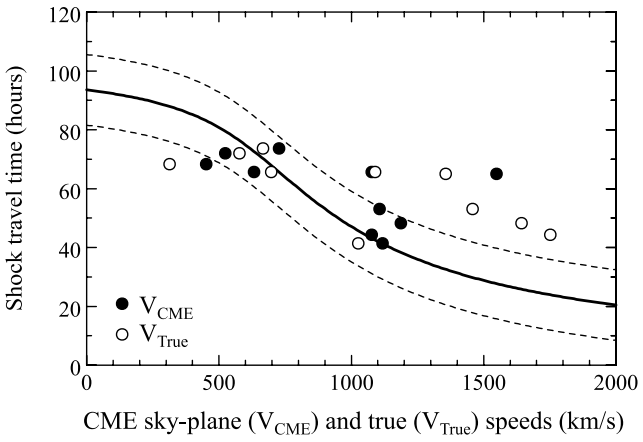

Figure 5. The solid circles are the events of sky-plane CME speeds, and the open circles are the events of corrected speeds.

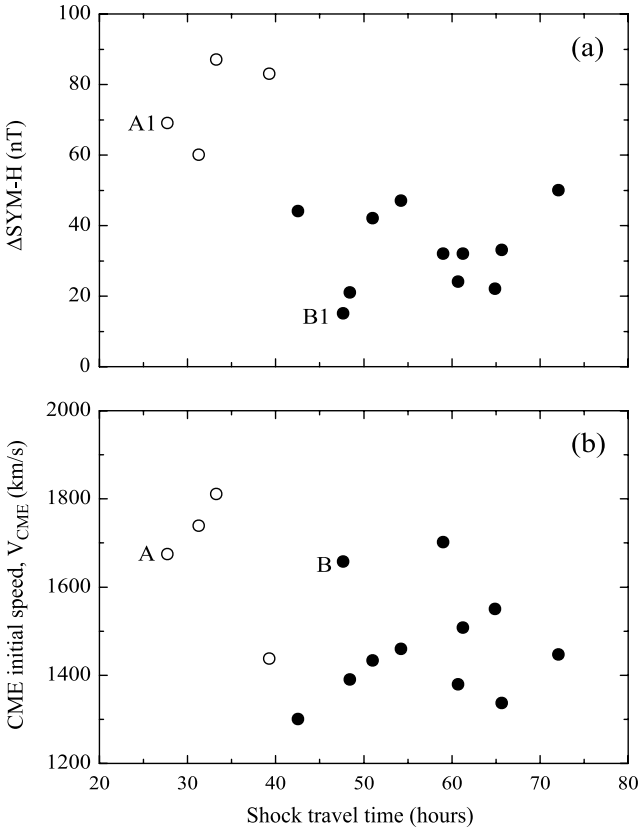

Figure 6. Scatter diagrams of (a) SC/SI strength versus IP shock traveltime and (b) V_{CME} versus IP shock traveltime for fast CMEs (V_{CME} >1300 km/s).

the CME initial speed. However, we do not exclude the possibility that the projection effect would be the main cause of the deviations from the ESA model. If a fast CME has narrow width and is launched toward the Earth, we expect small sky-plane speed of the CME, but it arrives early compared to the prediction based on the sky-plane speed. As shown in Figure 1c, there is a large scatter (~30 hours) in arrival time for slower (V_{CME} <700 km/s) and faster (V_{CME} >1300 km/s) CMEs. This large scatter would be explained by the projection effect. However, the projection effect cannot explain the positive deviation from the ESA model for faster CMEs (V_{CME} >1300 km/s) because the radial speed of CME is comparable to or larger than sky-plane speed.

[23] The IP shock events associated with the very fast CMEs on 14 July 2000 (V_{CME} = 1674 km/s), 8 November 2000 (V_{CME} = 1738 km/s), 4 November 2001 (V_{CME} = 1810 km/s), and 22 November 2001 (V_{CME} = 1437 km/s) lie closer to the ESA model prediction curve, which implies that the CMEs decelerate less than the other fast CMEs. The deceleration of the CMEs in the IP medium has been interpreted as a consequence of the interaction of the CME with the ambient solar wind. Therefore the deceleration is due to drag force acting on the CMEs [e.g., *Gopalswamy et al.*, 2001b; *Vršnak and Gopalswamy*, 2002]. The acceleration caused by drag force is given by

$$a = (\rho A C_D/M)(V_{SW} - V_{CME})|V_{SW} - V_{CME}| \qquad (1)$$

where C_D is the drag coefficient, ρ is the solar wind mass density, A is the cross section of CME, M is the mass of the CME, V_{SW} is the undisturbed solar wind speed, and V_{CME} is the CME speed [e.g., *Cargill*, 2004]. Thus the CMEs faster than the solar wind speed always experience a deceleration, which is proportional to the square of the difference in speeds between V_{CME} and V_{SW}. Equation (1) also says that the mass of a CME plays a significant role in determining the traveltime of IP shock. If CMEs travel toward the Earth with the same V_{CME}, massive CMEs are less decelerated because the deceleration is inversely proportional to the CME mass. They have short traveltimes compared with less massive CMEs.

[24] As we noted above, the four CME events lying close to the ESA model curve have short traveltimes and correspond to the four greatest SC/SI events (see Table 1) compared with other fast events. Figure 6 shows the amplitude of SC/SI events (ΔSYM-H) and V_{CME} larger than 1300 km/s versus the shock traveltime (the four events are marked by the open circles). There is a negative correlation between V_{CME} and shock traveltime, indicating that faster CMEs have shorter traveltimes. However, some events in similar V_{CME} range have a large scatter in traveltime. For example, events A and B in Figure 6b have similar V_{CME}, but event A arrived ~20 hours earlier than event B at the Earth. The amplitude of the SC/SI event (A1) corresponding to event A is much larger than the SC/SI amplitude (B1) corresponding to event B. Since the SC/SI event is caused by the sudden compression of the magnetosphere associated with a sharp increase in the solar wind dynamic pressure, determined by the solar wind speed and solar wind mass density, we suggest that event A is more massive than event B and that the negative correlation between the SC/SI strength and shock traveltime in Figure 6a may be due to not only V_{CME} but also the CME mass. The mass of CME can be estimated from the observed brightness of the photospheric light scattered by the coronal electrons. However, there is no simple way to obtain the mass estimation of halo CME [*Vourlidas et al.*, 2000]. Therefore it is difficult to examine directly the relationship between geoeffective CME mass and its deceleration. The CME mass is provided from the CME catalog [*Yashiro et al.*, 2004], but the halo CME mass is uncertain due to poor mass estimate. We do not use the CME mass parameter in this study.

[25] We note that the above argument of the CME mass contribution to the scatter of IP shock arrival time is applicable when the widths of the CME events in Figure 6 are comparable. If the width of event A is narrower than that of event B, the "true" CME speed of event A is faster than event B. Then, the fast CME (event A) accumulates more compressed material in front of it than the slow CME (event B) and drives strong SC/SI event compared with the SC/SI event corresponding to event B. As mentioned above, it is very hard to measure the "true" CME speed toward the Earth. Therefore it is not yet clear which of the factors, projection effect and CME mass/density, is dominant to make the large scatter in the IP shock traveltime in Figure 6. We expect that the STEREO mission will provide better tools for predicting the IP shock arrival time associated with Earth-heading CMEs with continuous coverage when it reaches a near-quadrature position.

[26] In summary, we examined the CME-associated IP shock traveltimes predicted by the ESA model based on a constant IP acceleration. The ESA model predicts 60% within ±12 hours. During solar maximum, we find that the deviations ($\Delta T = T_{obs} - T_{mod}$) of the shock arrival times from the ESA model show strong positive correlation with the CME initial speed (see Figure 2). This indicates that faster (slower) CMEs decelerate (accelerate) more than that expected in the ESA model. From the linear regression analysis, we obtained a linear fit to the relationship between shock traveltime and V_{CME}, $T = 76.86 - 0.02V_{CME}$, where T is the arrival time in hours and V_{CME} is the initial speed of the CME in kilometer per second. This linear fit predicts 74% within ±12 hours from the straight line. We observed that the fast CMEs corresponding to great SC/SI events have short traveltimes compared with other fast CMEs. This may be due to the CME mass; that is, massive CMEs are less decelerated and have short arrival times. However, we do not exclude the possibility of the projection effect for the large scatter in the IP shock arrival times. We suggest that the deceleration of the CMEs depends on not only CME speed but also CME mass and that two parameters, projection effect of V_{CME} and CME mass, should be considered for more accurate prediction. In the near future, we will further investigate the deceleration effect of CMEs. It would be interesting to examine the relationship between amplitude of SC/SI event and CME deceleration for the fast CMEs.

[27] **Acknowledgments.** This work has been supported by the MOST grants (M1-0104-00-0059 and M1-0407-00-0001) of the Korean government. The CME catalog used in this study is generated and maintained at the CDAW Data Center by NASA and the Catholic University of America in cooperation with the Naval Research Laboratory. SOHO is a project of international cooperation between ESA and NASA. The key parameter solar wind data of the ACE and WIND satellites are provided by the NASA's CDAWeb site. The SYM-H index data were provided by World Data Center C2 (WDC-C2) for Geomagnetism, Kyoto University.

[28] Amitava Bhattacharjee thanks the reviewers for their assistance in evaluating this paper.

References

Araki, T. (1994), A physical model of the geomagnetic sudden commencement, in *Solar Wind Sources of Magnetospheric Ultra-Low-Frequency Waves*, *Geophys. Monogr. Ser.*, vol. 81, edited by M. J. Engebretson K. Takahashi, and M. Scholer, p. 183, AGU, Washington, D. C.

Cane, H. V., and I. G. Richardson (2003), Interplanetary coronal mass ejections in the near-Earth solar wind during 1996–2002, *J. Geophys. Res.*, *108*(A4), 1156, doi:10.1029/2002JA009817.

Cargill, P. J. (2004), On the aerodynamic drag force acting on interplanetary coronal mass ejections, *Sol. Phys.*, *221*, 135.

Cho, K.-S., Y.-J. Moon, M. Dryer, C. D. Fry, Y.-D. Park, and K.-S. Kim (2003), A statistical comparison of interplanetary shock and CME propagation models, *J. Geophys. Res.*, *108*(A12), 1445 doi:10.1029/2003JA010029.

Gopalswamy, N., A. Lara, R. P. Lepping, M. L. Kaiser, D. Berdichevsky, and O. C. St. Cyr (2000), Interplanetary acceleration of coronal mass ejections, *Geophys. Res. Lett.*, *27*, 145.

Gopalswamy, N., A. Lara, S. Yashiro, M. L. Kaiser, and R. A. Howard (2001a), Predicting the 1-AU arrival times of coronal mass ejections, *J. Geophys. Res.*, *106*, 29,207.

Gopalswamy, N., S. Yashiro, M. L. Kaiser, R. A. Howard, and J.-L. Bougeret (2001b), Characteristics of coronal mass ejections associated with long-wavelength type II radio bursts, *J. Geophys. Res.*, *106*, 29,219.

Gopalswamy, N., A. Lara, P. K. Manoharan, and R. A. Howard (2004), An empirical model to predict the 1-AU arrival of interplanetary shocks, *Adv. Space Res.*, *36*, 2289.

Iyemori, T., and D. R. K. Rao (1996), Decay of the Dst field of geomagnetic disturbance after substorm onset and its implication to storm-substorm relation, *Ann. Geophys.*, *14*, 608.

Manoharan, P. K., N. Gopalswamy, S. Yashiro, A. Lara, G. Michalek, and R. A. Howard (2004), Influence of coronal mass ejection on propagation of interplanetary shocks, *J. Geophys. Res.*, *109*, A06109, doi:10.1029/2003JA010300.

McKenna-Lawlor, S. M. P., et al. (2002), Arrival times of flare/halo CME associated shocks at the Earth: Comparison of the predictions of three numerical models with these observations, *Ann. Geophys.*, *20*, 917.

Michalek, G., N. Gopalswamy, and S. Yashiro (2003), A new method for estimating widths, velocities, and source location of halo coronal mass ejections, *Astrophys. J.*, *584*, 472.

Moon, Y. J., et al. (2005), New geoeffective parameters of very fast halo coronal mass ejections, *Astrophys. J.*, *624*, 414.

Owens, M., and P. Cargill (2004), Predictions of the arrival time of coronal mass ejections at 1 AU: An analysis of the causes of errors, *Ann. Geophys.*, *22*, 661.

Srivastava, N., and P. Venkatakrishnan (2004), Solar and interplanetary sources of major geomagnetic storms during 1996–2002, *J. Geophys. Res.*, *109*, A10103, doi:10.1029/2003JA010175.

Vourlidas, A., P. Subramanian, K. P. Dere, and R. A. Howard (2000), Large-angle spectrometric coronagraph measurements of the energetics of coronal mass ejections, *Astrophys. J.*, *534*, 456.

Vršnak, B., and N. Gopalswamy (2002), Influence of the aerodynamic drag on the motion of interplanetary ejecta, *J. Geophys. Res.*, *107*(A2), 1019, doi:10.1029/2001JA000120.

Yashiro, S., N. Gopalswamy, G. Michalek, O. C. St. Cyr, S. P. Plunkett, N. B. Rich, and R. A. Howard (2004), A catalog of white light coronal mass ejection observed by the SOHO spacecraft, *J. Geophys. Res.*, *109*, A07105, doi:10.1029/2003JA010282.

K.-S. Cho, K.-H. Kim, and Y.-J. Moon, Korea Astronomy and Space Science Institute, Whaam-Dong, Youseong-Gu, Daejeon, 305-348, Korea. (kscho@kasi.re.kr; khan@kasi.re.kr; yjmoon@kasi.re.kr)